# Position and time sensitive photon counting detector with image charge delay-line readout

Achim Czasch[*a,b], Volker Dangendorf[c], James Milnes[d], Sven Schössler[a],
Ronald Lauck[c], Uwe Spillmann[b], Jon Howorth[d], Ottmar Jagutzki[a,b]
[a]Institut für Kernphysik, Universität Frankfurt, Max-von-Laue-Str. 1, 60438 Frankfurt, FRG
[b]RoentDek GmbH, Im Vogelshaag 8, 65779 Kelkheim, FRG
[c]Physikalisch-Technische Bundesanstalt, Bundesallee 100, 38116 Braunschweig, FRG
[d]Photek Ltd., 26 Castleham Road, St. Leonards on Sea, East Sussex, TN38 9NS, UK

## ABSTRACT

We have developed single photon counting image intensifier tubes combining position and time information read-out with at least 500x500 pixels and sub-nanosecond time resolution. This image intensifier type uses a resistive screen instead of a phosphor screen and the image charge pickup anode is placed outside the sealed tube. We present a novel delay-line anode design which allows for instance detecting simultaneously arriving pairs of photons. Due to the very low background this technique is suited for applications with very low light intensity and especially if a precise time tagging for each photon is required. We show results obtained with several anode types on a 25 mm image intensifier tube and a 40 mm open-face MCP detector and discuss the performance in neutron radiography, e.g. for homeland security, and the prospects for applications like Fluorescence Life-time Imaging Microscopy (FLIM), astronomy and X-ray polarimetry.

**Keywords:** photo-multiplier tube, MCP, image intensifier, delay-line, photon counting, 3d imaging, X-ray polarimetry, fast-neutron radiography, homeland security, scintillator read-out.

## 1. INTRODUCTION

Photo-multipliers with single photon detection capability are a commercially available tool for imaging at lowest light intensity and for photon-counting/time-of-flight applications. Nowadays, double or triple micro-channel plate (MCP) stacks are employed for providing sufficient gain for single photon detection across a few centimeters' diameter. In the VUV to soft X-ray area regime the bare MCP surface has a certain quantum efficiency, which can be enhanced by coatings. However, in the near-UV, visible and near-infrared wavelength regime, sealed photo-multiplier tubes (PMT) with a transparent photo-cathode on the entrance window are used [1].

In a standard MCP-PMT ("image intensifier") the photo-cathode converts photons into electrons. These photo-electrons are multiplied by the MCP and usually reconverted to photons by a phosphor screen, preserving the lateral position of the initial photon impact on the photo-cathode. Such image intensifiers are usually read out by CCD devices. If equipped with double- or triple-stacked MCP operated in saturation, single photons can be imaged and counted, but the time resolution is very coarse, i.e. limited to a few milliseconds by the CCD frame rate.

If precise timing information is required the phosphor screen must be replaced by a metal anode for electronic signal pickup, which can be partitioned into many segments for providing at least coarse information on the position [2]. Such devices are applied to count and determine the arrival time of single photons with precision of tens of picoseconds, e.g. for time-of-flight measurements.

By correlating a phosphor screen/CCD read-out with electronic time-signal pick-up or by pulsing the photo-cathode, the usually poor time resolution of CCD read-out is increased into the few nanoseconds' regime while maintaining a high position resolution. However, then either the detection rate is limited by the CCD frame rate, or the

[*]czasch@atom.uni-frankfurt.de; phone +49 69 798-47018; fax +49 69 798-47107

duty cycle for continuous detection becomes very poor due to the limited pulse repetition rate, technical constraints which are difficult to overcome [3].

There are only a few commercially available single photon detectors which can simultaneously provide time resolution with nanosecond precision and imaging with more than 100x100 pixels for a quasi-continuous photon flow [4,5]. These photo-multiplier tubes use the so-called resistive anode (RAE) in place of a phosphor screen/ metal anode to encode the position by electronic signal pick-up from corner contacts of a specifically shaped resistive layer anode. This technique allows true "3d-detection" (2d-position and time) of photons with high temporal and high spatial resolution for individual photons. However, the electronic chain of the RAE involves "slow" electronic circuits, which principally limit the achievable count rate: There is a trade-off between position resolution, detector size and detection rate. Therefore, it would be beneficial employing other 3d-imaging anode concepts developed from open-face MCP detectors also for sealed MCP-PMT, e.g. the delay-anode, a technique which does not compromise detection rate versus resolution or detector size and even allows detecting pairs of simultaneous photons at different positions [6].

Incorporating superficially structured anodes like wired delay-line arrays into image intensifiers is a difficult task and not suitable for mass production because the production process involves harsh baking processes and reduces the material choice. Nevertheless, scientific prototypes with up to 75 mm active diameter demonstrated that delay-line read-out for single photon detection gives superior performance for specific detection tasks and might become a general alternative to standard CCD designs as soon as tube production can be optimized and the electronic read-out circuits can be further improved [7-9].

Applications for such photon counting detectors are found in astronomy or similar low photon rate survey tasks, Laser-Induced Fluorescence Life-time Imaging Microscopy (FLIM) [9,10] or spectroscopy (LIF) and scintillator imaging for X-ray detection [5] and fast neutron radiography [11], which will be exemplarily discussed in more detail later in this paper. Demands for homeland security and fast tracking of UV sources can benefit from these techniques.

We propose a simplified photo-multiplier design which is suitable for mass production at comparatively low costs which can be equipped with a variety of specific read-out electrodes *outside* the sealed tube. Among those are delay-line or other superficial pick-up structures like pixel arrays, Wedge&Strip/Vernier electrode patterns [12-15] or any other "antenna" that can register the image charge pulse from the electron cloud collected on the resistive layer inside the tube.

In this paper we will present and discuss novel delay-line read-out electrodes on multi-layer PCBs by showing their performance on such a novel-technique photo-multiplier tube and on an open-face MCP detector suitable for VUV/X-ray or particle detection. We will demonstrate that single photon detection devices for visible wavelength with a position resolution of at least 500x500 pixels, sub-nanosecond time precision with negligible (or even no) dead-time between individual photon hits and large open area can now be produced economically. We conclude with an outlook on the perspectives of these detector types in becoming the "ideal" single-photon detector in the future.

## 2. THE RESISTIVE-SCREEN PHOTO-MULTIPLIER TUBE

Image intensifiers with phosphor screen and optical read-out are an industrial standard product and can be produced very economically in specialised facilities. However, introducing major changes to the tube design (like introducing a dedicated read-out board into the high vacuum tube) usually requires major modification to the production facility and makes these tubes quite expensive. Furthermore, once built and sealed, there is no chance to modify or optimize the read-out electrode unless one starts producing a new tube.

Therefore, in 1999, we have proposed and patented a method to minimize the changes required to a commercial image intensifier and simultaneously permitting a very flexible design of the read-out electrode [15]. This method, originally proposed by Battistoni *et al.* [16] and extensively used in various applications with gaseous detectors, uses an anode (screen) with a very high surface resistance, which replaces the usual metal-coated phosphor screen of a standard optical read out image intensifier. This resistive layer with a typical surface resistance of > 1 $M\Omega_{\square}$, acts as an electromagnetically transparent window for the signal of the traveling electron cloud as it propagates from the last MCP to the resistive screen.[*] While in gaseous detectors these layers are made of resistive lacquer based on carbon and plastic material, the high purity requirements in vacuum image intensifiers demand for non-outgassing materials like

[*] This type of resistive screen should not be mistaken for the RAE, which also uses a kind of resistive layer but with about three orders of magnitude lower area resistance and conductive signal pickup from the layer (i.e. inside the tube).

Germanium. Fig. 1 shows a sketch of such a Resistive-Screen Photo-Multiplier Tube (RS-PMT). Apart from the resistive screen and a possible thinner (and not necessarily optically transparent) output window it is very similar to a commercial image intensifier with a double or triple MCP stack. The typical performance parameters of the photo-cathode are the same, e.g. choice of cathode material, its quantum efficiency and dark noise properties. Lifetime, mechanical properties (rigidness) and the operability at low temperature are not affected by the structural change.

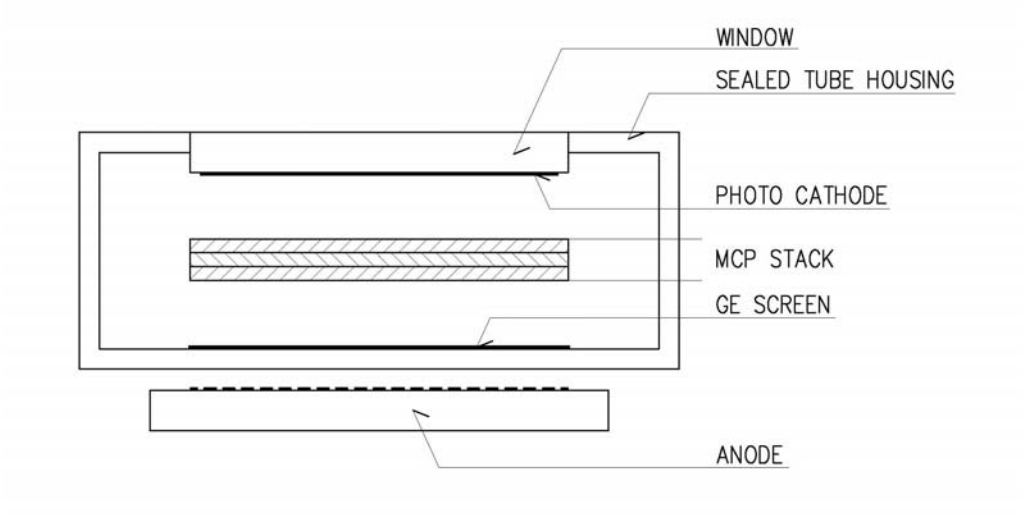


Fig. 1: RS-PMT tube with resistive screen (here: Germanium layer) replacing the phosphor screen of a conventional image intensifier. The position information is obtained by a dedicated pickup electrode (anode) outside the tube housing.

The resistive layer (e.g. of Germanium) is deposited directly on the vacuum side of the output window (glass or ceramics) of the intensifier. The read-out board is mounted outside the tube in close contact to this window. The spacing between the traveling charge cloud inside the tube and the separated read-out electrode outside causes a geometrical spread of the induced signal on the read-out board. For MCP-based image intensifiers but also for gas detectors like GEMs or RPCs (resistive plate chambers) this is of great benefit because it allows using rather coarse read-out structures for a delay-line read-out, e.g. strips of a few millimeters' pitch,. In recent years several read-out techniques using this resistive screen technique for image intensifiers were reported in literature [12-14].

Also theoretical studies calculating the induced charge distribution are available in literature [17-19]. We have experimentally studied and optimized the relevant parameters, including the geometrical distribution of the induced signals and its dependence from the distance between resistive layer and pickup electrode and the required surface resistance of the layer for maximum signal transmission. Furthermore, we studied the geometrical structure of the signal pickup strips of the read-out board. Detailed results of these measurements will be published elsewhere. It turns out that a strip pitch of 2 mm on a read-out board is a good approximation of the ideal value needed for a read-out of the image charge through a 2 mm thick ceramic substrate. Although smaller strip pitch distances would be desirable, the output windows of image intensifiers have to be of a certain thickness usually above the optimal value, due to the requirement of a stable housing for the vacuum inside the tube. Nevertheless, future developments must address this issue and an optimization of the material and its thickness is unavoidable especially for proposed larger devices with > 50 mm sensitive diameter.

## 3. DELAY-LINE READ-OUT FOR THE RS-PMT

Early work on the read-out of RS-PMT with Wedge&Strip anodes, adopted from open-face MCP detectors, stated a position resolution between 30 and 40 micron (pixel size) on a 25 mm RS-PMT produced by Proxitronic GmbH in Bensheim, Germany [13]. In order to increase the count rate these early tests were followed by designing delay-line anode (electrode) structures suitable for image charge pick-up, which is similar to a delay-line anode proposed earlier by Eland for an open-face MCP detector [20]. The position read-out electrode is a double-layer or multi-layer standard

printed circuit board (PCB) with orthogonal strip structures on both sides connected either by a meander-shaped track (i.e. delay-line) [15] or via an LC delay-line as will be described in more detail.

Fig. 2 shows the front- and backside structure of an optimized read-out electrode for a 0.3 mm thick FR4 board. The strips, whose shapes resemble a chain of diamonds, are copper-etched and have a pitch of 2 mm. The front side (Fig. 2a) has much smaller pads to avoid electromagnetic shielding of the back side (b) and to ensure equal signal amplitudes on both sides of the read-out board. The diamond-shaped pads of the front side are located in the open areas between the pads of the back side. The structures overlap only at the intersections of the thin strips connecting the diamonds, minimizing capacitive coupling between both sides of the board. The rows are connected to a delay-line for each dimension.

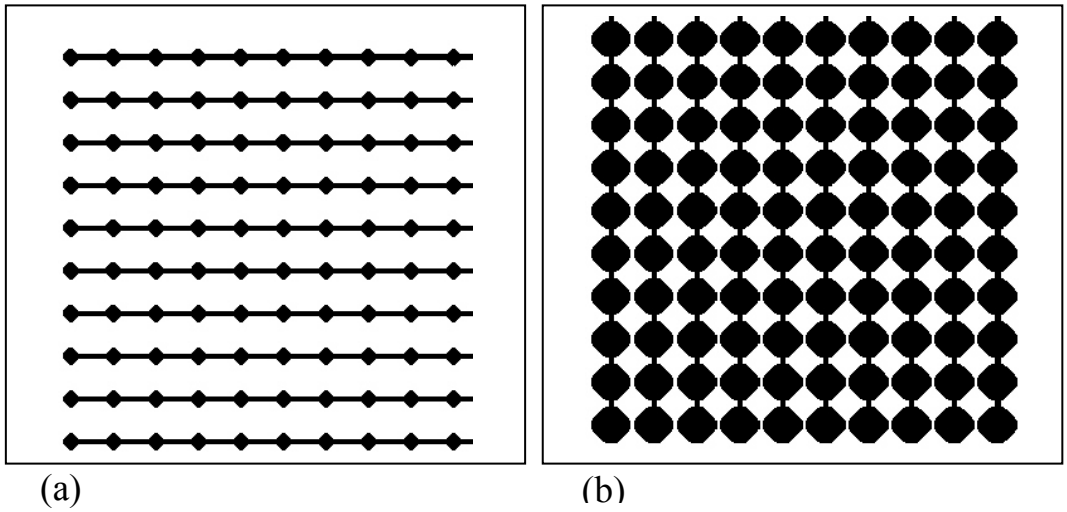


Fig. 2: sections of the strip structure of the front (a) and back (b) side of the position read-out board. The strips have a pitch of 2 mm and run in orthogonal directions.

Similar pick-up patterns in combination with meander-shaped delay-lines connected to the rows gave good results [15]. Still, we have now concentrated on LC delay-lines because an LC delay-line potentially allows easier design handling, impedance matching and a larger delay per pitch (yielding an increased position resolution with low signal damping). However, such delay-lines may have a less linear response due to tolerances in the electronic components.

Fig. 3 shows the rear side of a delay-line anode for read-out of RS-PMT with < 50 mm detection diameter. Coils of 290 nH connecting the strips and capacitors to ground (27 pF) form a LC delay-line with nominal 2.5 ns delay per tap and 100 Ohms impedance, which is transformed to 50 Ohms at the outputs. Vias from the front side allow placing both delay-lines on the substrate's rear side, leaving a flat front surface for close contact with the RS-PMT rear wall. It is also possible to "fold" the delay-line circuit chains into the third dimension in case of lateral space restrictions.

The four contacts were connected via 50 Ohms coax cables to the inputs to an *ATR19* amplifier and constant fraction discriminator (CFD) unit [21] and the time sequence of the timing outputs was analyzed by a *TDC8HP* time-to-digital converter [21]. In some of the tests other (similar) amplifier and CFD units were used to obtain position and time information. The electronic chain for delay-line detectors has been described elsewhere (i.e. in [6] or references therein). In short, the time sequences of signals from the two ends of both delay-lines are recorded relative to the MCP signal, which is capacitively picked up from an MCP contact and likewise processed with an amplifier and CFD. The MCP signal may serve as a time marker for the photon detection relative to an external trigger.

The time difference of two delay-line signals from opposite ends is proportional to the position of the detected photon in the respective lateral dimension. Note that the position resolution is not limited by the delay-line pitch but only by the time resolution of the electronic circuits. With nowadays' TDC circuits it is possible to achieve a timing precision of 25 ps or better at a particle rate of 350 kHz or more. The dead-time after each detection event can be as small as 10 ns (or smaller) so that even bursts of particles can be detected (high short-term rate). This gives a major advantage over competing single photon read-out concepts like Wedge&Strip or RAE based systems.

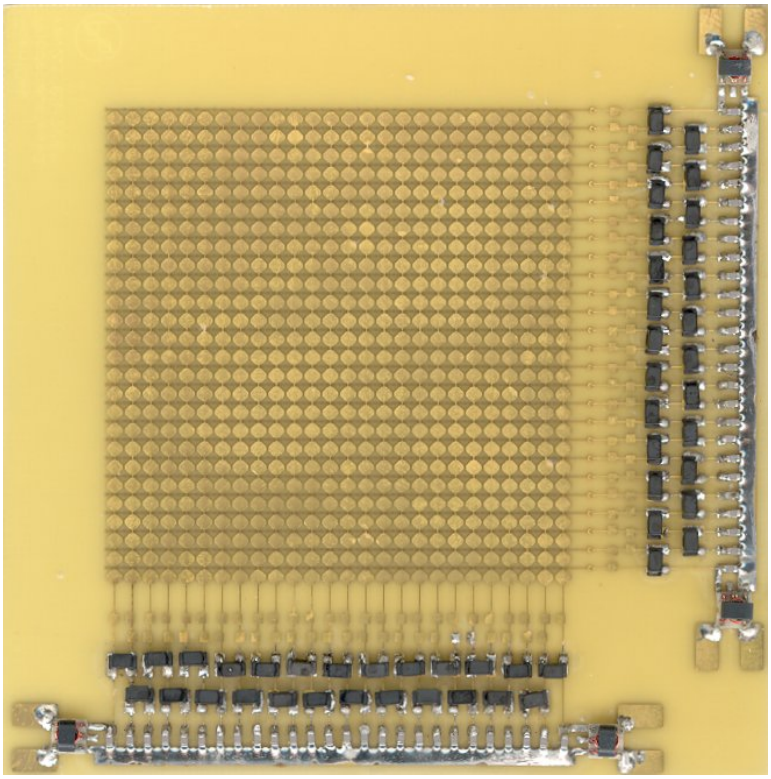

Fig. 3: Rear view of a 50 mm delay-line read-out structure for RS-PMTs. The LC sequence on the right side is connected by vias to the front side strips (see fig. 2). The LC sequences form delay-lines with 2.5 ns tap per pitch (2 mm).

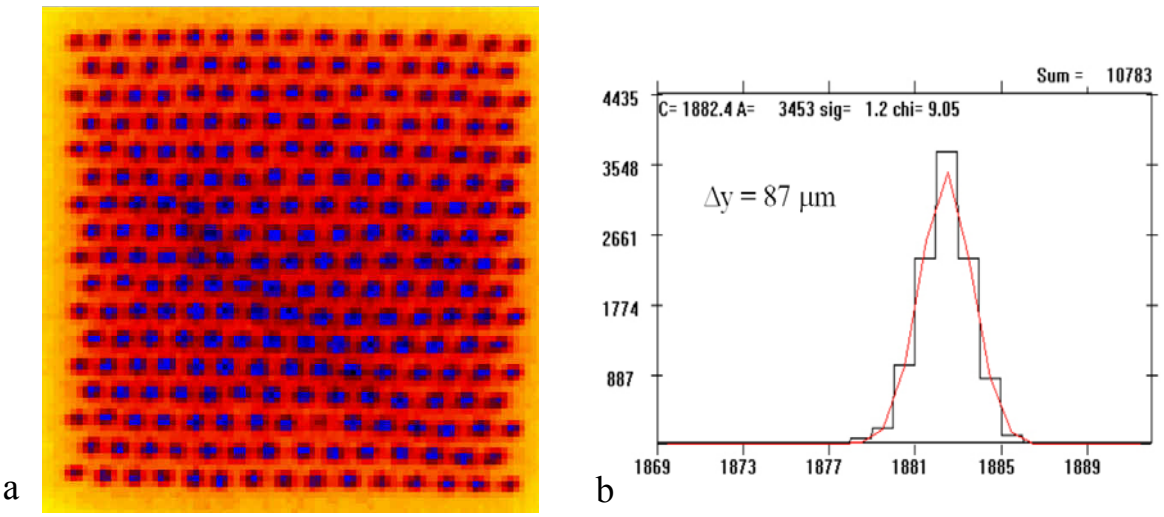


Fig. 4: Image (linear z-scale) of an optical mask measured with the RS-PMT and delay-line read-out (a). The mask on the RS-PMT is illuminated by a pulsed $H_2$-lamp. The distance between the holes of the mask is 0.7 mm and the holes' diameter is 0.3 mm. b) shows the projection of a tiny pinhole. The width of the peak corresponds to 87 μm (FWHM). The resolution on the back side of the board is slightly worse (116 μm FWHM).

Fig. 4 shows imaging results from such a delay-line read-out board on a 25 mm RS-PMT, the same as used as in [13]. (a) is an image obtained from an printed optical shadow mask, illuminated by a pulsed hydrogen lamp. (b) shows the cut through a single pinhole with same illumination. The position resolution obtained with this device and described read-out is 87 micron (FWHM). The digitization of the TDC corresponds to a pixel size of about 30 micron. The position resolution on the back-side of the board is slightly worse (116 μm FWHM). These results are comparable to those obtained with Wedge&Strip anodes. Tests planned for the near future on a 40 mm RS-PMT equipped with high gain MCP will show the resolution limits of the technique.

For determining the linearity of this read-out technique we performed tests of the same read-out board on an open-face RS-MCP detector with very similar design. The major difference from Fig.1 is the absent solid window in front of the MCP to allow for direct particle and VUV/X-ray detection. The functional elements (resistive screen on a ceramic substrate behind a chevron MCP stack) are essentially the same. The position resolution for this assembly was also estimated to be 100 μm or smaller. However, more accurate measurements are still pending. Fig. 5 shows the imaging response of a 40 mm open-face detector to a hexagonal mask with 1 mm pitch, illuminated with slow ions. Existing RS-PMTs show a (software-correctable) radial distortion [13]. Therefore it is difficult to independently determine imaging linearity deviations which may arise from the read-out board alone, i.e. from tolerances of the capacitors and coils forming the delay-line.

In order to determine linearity deviations from an imperfect RC-delay line, we have designed a "self-correcting" delay-line array based on the principle of the so-called Hexanode, a three-layer structure with redundant signal pick-up properties: Three equal delay-line structures are placed at 60° relative angles and form a redundant u/v/w coordinate system in such a way that the signals from any two delay-lines are sufficient to determine the position in x and y dimension. The main purpose of the Hexanode array is improving the multi-hit performance of a detector, i.e. to allow a position and time recognition even for simultaneously arriving pairs of particle/photons [22].

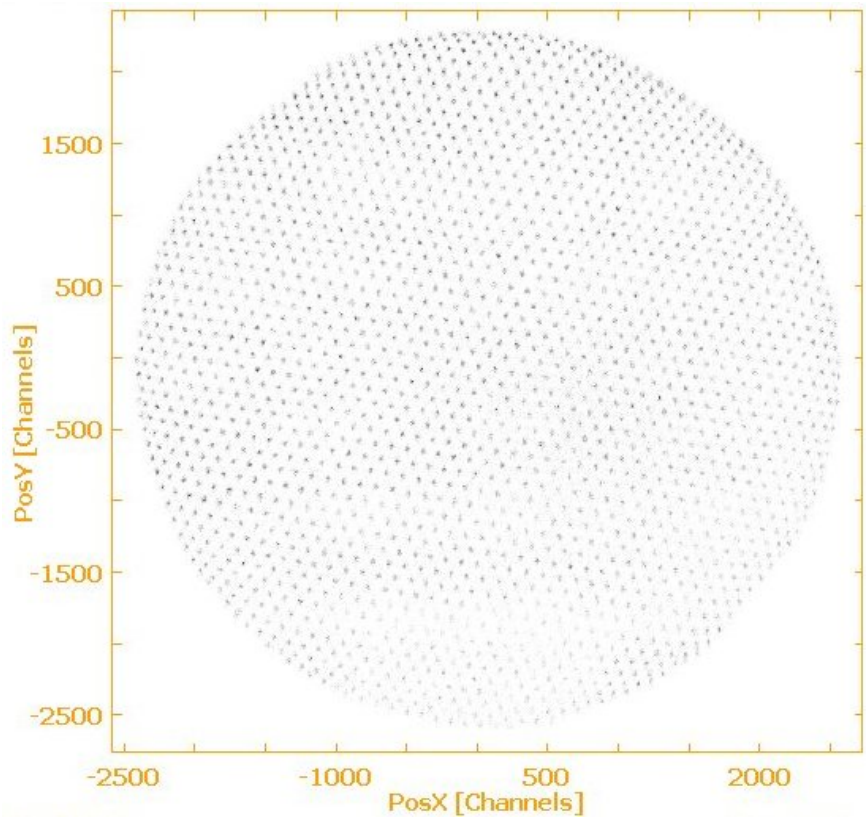


Fig. 5: Imaging response (linear grey scale) of a 40 mm open-face RS-MCP detector to a hexagonal mask with 1 mm pitch, illuminated with slow ions. The hole pattern is produced by a focussing effect of the ions through the hexagonal mask onto the MCP.

Designing a Hexanode capable of image charge read-out requires a thin multi-layer PCB with at least three strip layers. The distance between layers should be small to minimize effects of signal damping as a function of distance from the Ge-screen. Also, the pick-up structure on the strips should be chosen to (ideally) produce equal signal sharing on the layers. Fig. 6 shows a Hexanode for image charge read-out. The mean pulse height from the first layer turned out to be twice as much as the heights obtained from the other two although the area of the first layer was minimized. However, the pulse height on all layers was sufficient to allow for an equal performance of all layers.

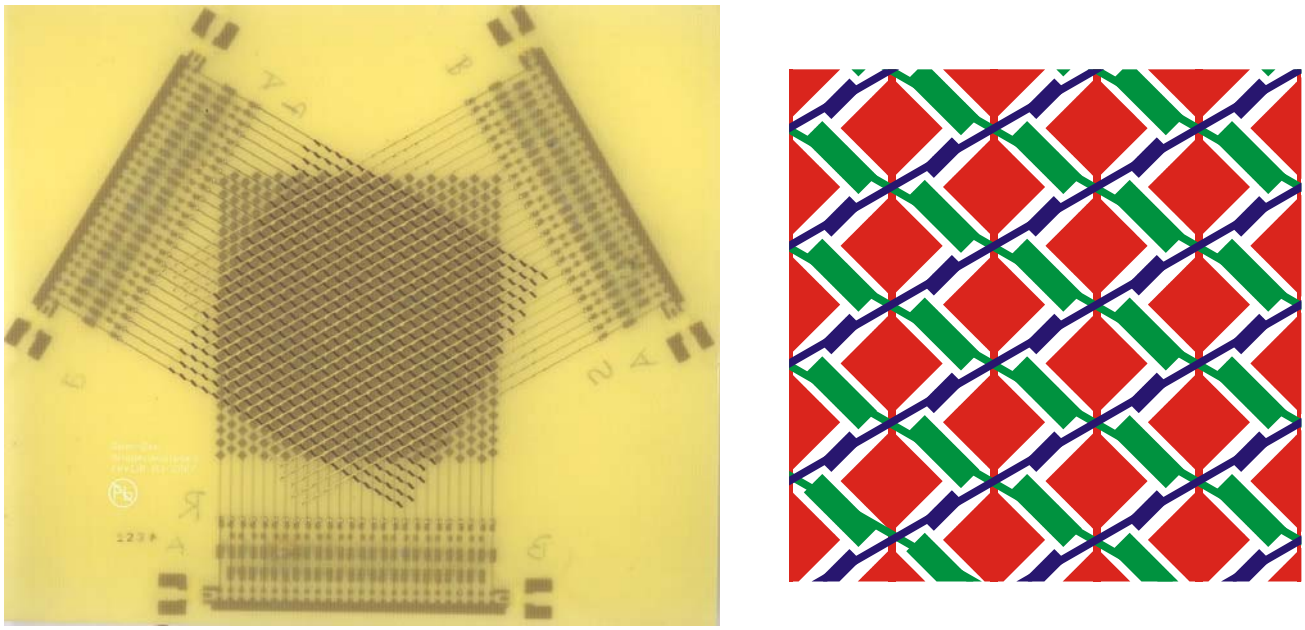

Fig. 6: Hexanode for 40 mm RS-PMT-type detectors. The substrate is a 4 layer PCB with about 115 micron spacing between the layers. The strips have 2 mm pitch and the different pick-up areas shall account for the shadowing and damping of the image charge on the three different delay-line layers. The largest structures (diamonds) are on the strip layer farthest from the resistive screen and define the u-coordinate. The layer with the smallest pick-up area is on the front layer (w-coordinate), the v-layer (with medium-sized pads) is in between. The strips are connected via LC delay-lines of 2.5 ns per pitch placed on the rear layer.

By using such a Hexanode, x/y positions of a photon/particle can be derived from the information of u/v or v/w or w/u layer pairs independently, disregarding the information from the respective third layer. Example: if we consider the u-layer, with the largest (diamond-shaped) structures, to be aligned with the physical x-direction, it is possible to determine the x-dimension of a photon/particle impact either by the position on u-layer or by vector addition of the information from both other layers v and w, entirely disregarding information from the u-layer: $\mathbf{x} = \mathbf{u} = -(\mathbf{v} + \mathbf{w})$. A similar consideration can be done for the y-direction, for a detailed discussion please refer to [22]. Only if the three delay-line layers have a perfectly linear response then all three different computation options will lead to exactly the same x/y position for any detected single photon/particle. Linearity deviations of the individual delay-lines will thus result in relative positions errors from the different computations.

Figure 7a (right curve) shows a histogram of position errors calculated from different layers for a homogenous sample of positions integrated over the whole detection area. The detector was illuminated like in Fig. 5. The full spectrum of the linearity function, showing a half width of about 0.2 mm, is not yet fully understood. However, part of these deviations can be attributed to non-linearity of the LC delay-lines.

If only projections of deviations to a certain coordinate are considered, deviations originating from LC-chain tolerances can be attributed to the individual layers: As an example, Fig. 7b shows the deviation in the x-position of a certain photon/particle measured only by the u-layer compared to determining this same photon/particle's x-position with information from the v- and w-layers.

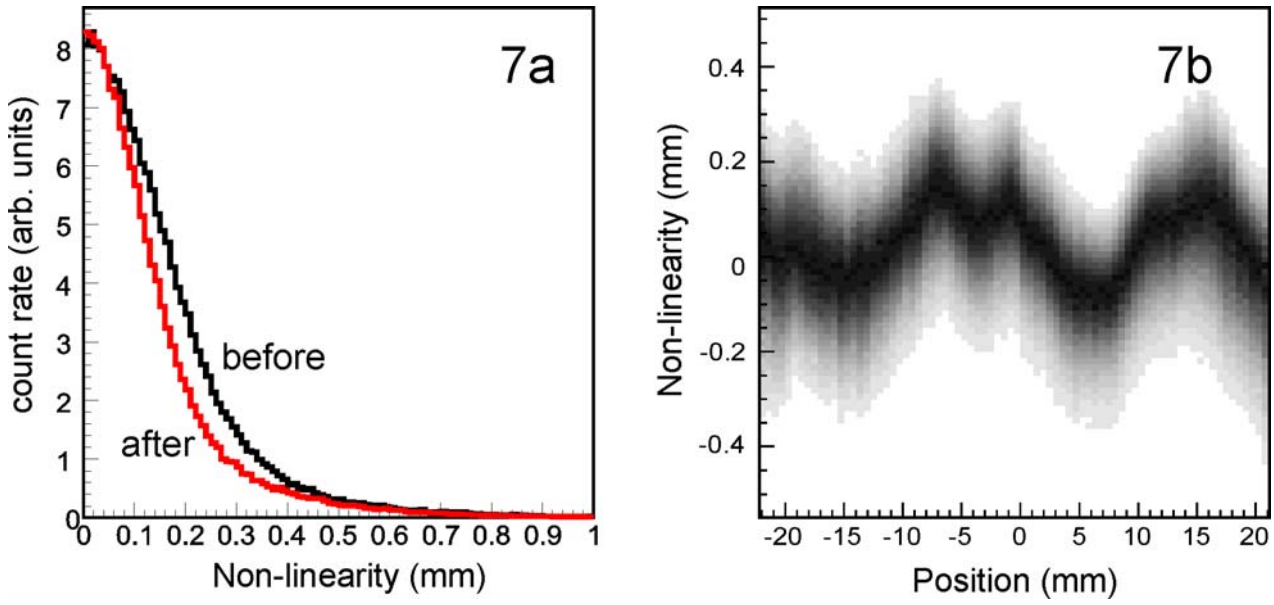


Fig. 7: Position deviations calculated from the different Hexanode layers integrated over the whole detection area. 7a shows a histogram of the deviations before and after a correction procedure from calibrating each delay-line by comparing its position measurement to values obtained from the two other layers (Fig. 7b, for u-coordinate). The detector was illuminated like in Fig. 5.

The structure found in Fig.7b as function of u-coordinate (i.e. x-coordinate) can be mostly attributed to the non-linearity function of the u-layer because a fixed position on the u-layer corresponds to varying positions in the v- and w-layers (only the sum **v** + **w** is constant for a specific u position). Linearity errors from the v- and w-layers along the x-direction are averaged and can only contribute to the finite thickness of the line in Fig. 7b. Thus it is possible to correct the non-linearity of the u-layer by a function obtainable from the line in Fig. 7b. Likewise, the non-linearity of the v- and w-layers can be corrected. As a result of this calibration procedure Fig. 7a (left curve) shows the histogram of position deviations calculated from different layers integrated over the whole detection area after linearity correction of all layers. The remaining non-linearity might be caused by the position resolution limits in this measurement.

Note, that this "self-calibrating" linearity correction does not require a calibration mask. It can be done with any more or less uniform illumination of the detection area of interest and it is not affected by other image distortions, e.g. a radial distortion from the RS-PMT design.

As a result, when using a Hexanode any linearity deviation caused by imperfect LC delay-line arrays can be intrinsically corrected without the need of calibration measurements with a test mask. This eases the production of such anodes because no special care in component selection and placing accuracy is necessary and no extensive mask calibration procedures are required. Once the linearity calibration parameters of a Hexanode are specified, the remaining distortion characteristics of a specific RS-PMT detector can be determined. This still requires a calibration mask, like the correction of a standard delay-line array with only two layers.

Fig. 8a shows the imaging response after a radial correction procedure for the 40 mm RS-PMT. The radial correction function (solid line in b) was determined from the image response to a calibration mask (as used in Fig. 5) after LC-delay-line non-linearity correction (b). The deviation due to intrinsic properties of this RS-PMT design can be as big as 1 mm at the outer image diameter, but it can be corrected. Fig. 8c shows the remaining linearity deviations after the correction in an area within 40 mm of diameter. The non-linearity is in the order of the position resolution. While the radial correction is certainly necessary, the non-linearity contribution of the LC-delay-line may be neglected because those errors are small (see Fig. 7b) although no special care of L/C chip selection or accurate placement or soldering procedure was applied. This can justify using the "simpler" two-layer geometry as in Fig. 3.

Of course the main idea of producing a Hexanode array for RS-PMT is not only its intrinsic linearity correction property. There are applications where a simultaneous detection of two photons is of great interest. In the following chapter we present a practical application of a RS-PMT with delay-line read-out in pulsed fast-neutron imaging for

explosives and drug detection and formulate the idea of measuring the polarization of X-rays with the help of scintillator imaging with RS-PMT equipped with a Hexanode.

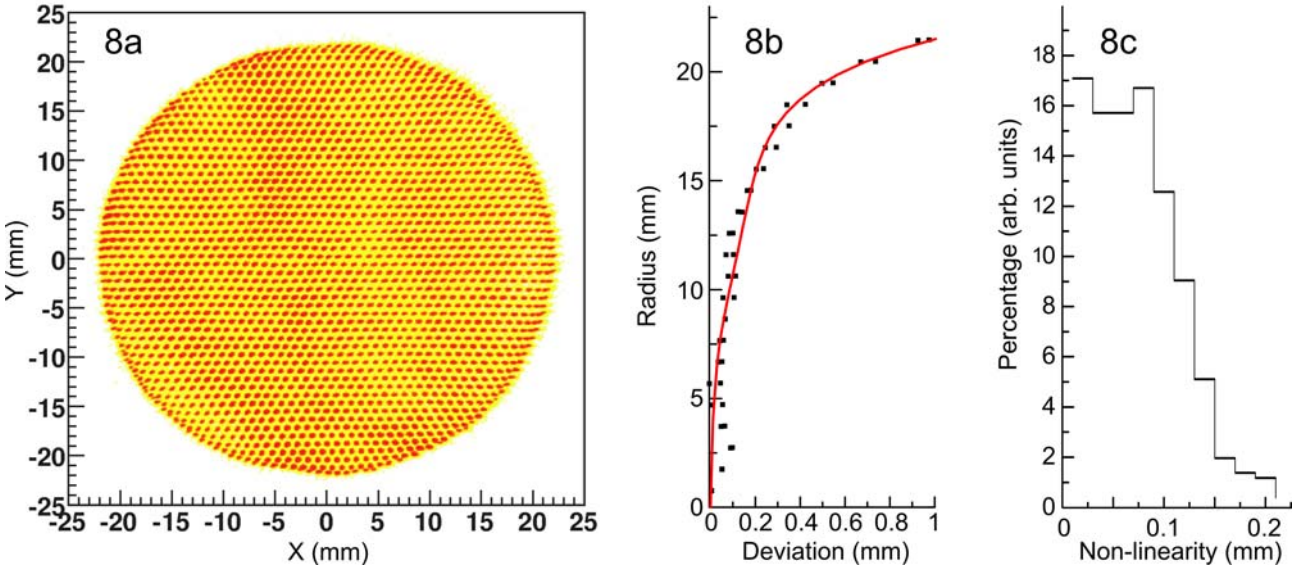


Fig. 8: Left image (a) shows the 40 mm RS-PMT imaging response (logarithmic z-scale) to a calibration mask after LC-non-linearity correction and after applying an additional polynomial radial correction function (solid line in Fig. 8b). Right image (c) shows a histogram of remaining linearity deviations in an area within 40 mm of diameter.

## 4. READ-OUT OF SCINTILLATOR FOR X-RAY POLARIMETRY AND FAST-NEUTRON RADIOGRAPHY WITH 3D-IMAGING RS-PMT AND DELAY-LINE ARRAYS

The 3d imaging of photons is not limited to experiments where single photon detection from a sample is the subject matter. MCP-PMTs of varies kinds are used to register secondary photons emitted from scintillating material. A commercial X-ray imaging device is already using this technique: a scintillator plate is placed on the entrance window of an image intensifier [5]. Alternatively one can use optics to focus a scintillator plate to an image intensifier positioned elsewhere. This is especially important if the reproduction scale shall be varied or if the image intensifier may suffer from the direct irradiation, as in fast-neutron radiography.

Energy-resolved fast-neutron radiography is a promising method for element-sensitive imaging of low-Z materials, which cannot be resolved by standard X-ray or thermal-neutron techniques. Fast neutrons have a high penetration power and, due to the specific structures (resonances) in the neutron cross sections of elements like C, N or O in the MeV range, this method may be used to resolve the spatial distribution of those elements, e.g. in air cargo containers or luggage. A prerequisite for this application method is the possibility of obtaining neutron transmission images in selected narrow energy ranges. One method is spectroscopic 3d-imaging in pulsed, broad-energy neutron beam illumination by applying time-of-flight (TOF) methods for energy selection [11,23,24].

Fig. 9 shows a schematic view of such a detector and the element-sensitive imaging which can be obtained. The neutron converter is a 10 mm thick BC400 scintillator slab with a surface area of 20 x 20 $cm^2$. The sample (not shown in Fig. 9) is placed in front of the scintillator. An optical system projects a circular area of about 10 cm in diameter towards the image sensor. The optical read-out consists of a flat 45$^o$ reflection mirror, a large aperture lens with a focal length of $f$ = 120 mm and a focal/diameter ratio of 0.95 (F-number) and the RS-PMT (the same as used in Fig. 4) as image sensor. Individual neutrons produce photons in the scintillator. Some of the photons are captured by the optics and focused onto the RS-PMT via the mirror and lens system. The TOF measurement reveals the energy of the neutron. Since the energy spectrum of the neutrons is dependent on the elements in the irradiated up-stream sample, one can achieve element sensitive imaging by this method. The reason for installing the mirror is to save the detector from radiation damage and activation. Such a mirror would not be necessary for less destructive primary beams.

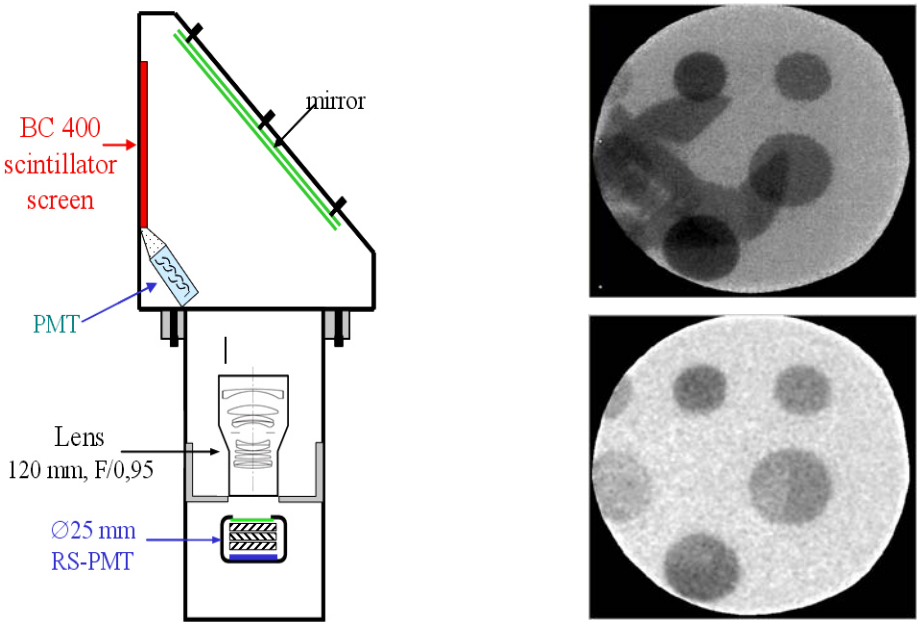


Fig. 9: Schematic view of the element-sensitive neutron imaging system with a RS-PMT. A pulsed 1 – 10 MeV broad-energy neutron beam irradiates a sample made up of carbon chunks and a steel wrench. The RS-PMT detects secondary photons from the scattered neutrons by imaging the scintillator plate. The radiographic image of the sample is shown in the picture up left. Using the TOF information, an element-sensitive image showing only the carbon chunks is obtained.

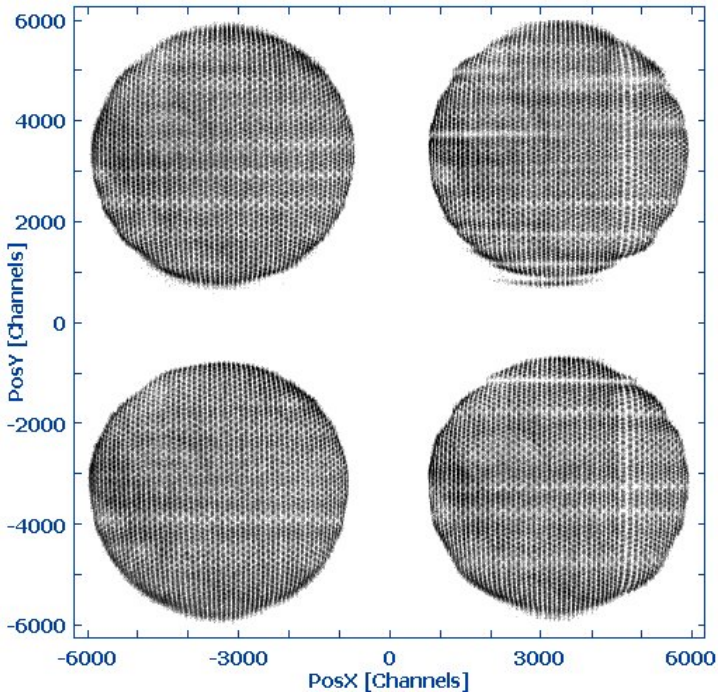


Fig. 10: Imaging property of 105x105 mm² delay-line array prototype with LC delay-line. A 40 mm RS-PMT-type detector was illuminated like in Fig. 5 and the anode was placed at different positions consecutively while acquiring data.

A complete neutron imaging system would consist of a matrix with many elements of such scintillator/lens/RS-PMT assemblies for achieving a sufficiently large area. Here the use of the novel RS-PMT would be of great advantage due to its potential for economical mass production. By equipping square-shaped RS-PMT of about 50x50 mm² which are already commercially prototyped [2] and placing several of these densely packed on a large delay-line anode one could produce large-area sensors at comparably low costs. Tests on a 105x105 mm² delay-line array demonstrated the feasibility (see Fig. 10), although a next version will use a different LC delay-lines with smaller total delay in order to avoid image artifacts caused by signal damping. It is possible to combine four of these delay-lines with 16 square shaped 5x5 cm² RS-PMT to a sensor array measuring 20x20 cm² with a large active area ratio.

The technique of utilizing 3d-imaging via scintillator read-out by RS-PMTs is not limited to fast neutrons. Other energetic particles create secondary photons as well and also X-rays can be imaged likewise. Especially introducing the Hexanode for RS-PMT read-out and thus being able to determine the positions of simultaneously arriving photons, one could for example build up an instrument for measuring the polarization of hard X-rays.

As has been described by Suzuki *et al.* [25], a combination of segmented scintillator and multi-anode PMT can be used to determine the polarization of hard X-rays. By measuring the relative positions of a Compton scattering and the absorption of the scattered X-ray in the scintillator one can determine the polarization vector of the X-ray. Since both interactions create photons within less than a nanosecond at the two scattering positions, a RS-PMT equipped with a "multi-hit" Hexanode read-out could image such an event: both scattering positions are registered in coincidence, independently for each X-ray. Here, a single RS-PMT with Hexanode can be an alternative to segmented PMT arrays.

## 5. SUMMARY AND OUTLOOK

In summary, we could show that RS-PMT photon counting detectors equipped with delay-line anodes are a mature technique for 2d- and 3d-imaging tasks. RS-PMTs of several sizes are meanwhile commercially available products from several manufacturers and the delay-line read-out concept is well-matured and also offered commercially. The robust tube design will allow for a qualification for harsh environment and the imaging performance is not influenced by strong magnetic fields.

Typical performance parameters are at least 500x500 pixels of position resolution with simultaneous timing precision of < 1 ns for individual photon counts at rates up to 350 kHz currently. The Hexanode read-out option allows the detection of simultaneously arriving photon pairs and provides an intrinsic control of the image linearity. Final limitations on the position and time resolution as a function of the count rate and the maximum possible image size are still to be determined.

We demonstrated how RS-PMTs with delay-line read-out can be used as time- and position-sensitive (3d-)cameras for imaging fluorescence screens for fast neutrons or other energetic particles/photons. Such cameras can be stacked to allow for a large sensor area and can be produced economically due to the simple design of the sensor head and read-out circuits.

While RS-PMT detectors with delay-line read-out are already in use for Fluorescence Life-time Imaging Microscopy (FLIM) and fast-neutron radiography there is large potential for other applications, e.g. in the fields of X-ray detection/polarimetry, astronomy, fast UV-source tracking and homeland security. This technique can also be used in combination with open-face MCP detector for advanced VUV and particle (e.g. electron) imaging and spectroscopy.

Next-generation TDC circuits already in production will allow increasing the photon/particle detection rate to more than 1 megacounts/s. Due to the superior imaging properties of pulse counting methods it is desirable using such detectors for pure imaging applications, too: photon/particle counting methods do not show saturation effects at long exposure times and yield better image contrast and dynamics than usually obtainable with intensified-CCD approaches. This may make this photon/particle counting&imaging technique superior over standard approaches even if no timing information is needed. At least this seems principally feasible for detection rates of up to 10 megacounts/s.

## REFERENCES


1. see for example *http://www.proxitronik.de* or other manufacturers' home pages
2. see *http://www.burle.com*
3. V. Dangendorf, A. Breskin, R. Chechik, G. Feldman, M. B. Goldberg, O. Jagutzki, C. Kersten, G. Laczko, I. Mor, U. Spillmann, D. Vartsky, *Nucl. Instrum. Meth.* A 535, 93 (2004)

4. see *http://www. quantar.com*
5. see *http://www.photek.co.uk*
6. O. Jagutzki, V. Mergel, K. Ullmann-Pfleger, L. Spielberger, U. Spillmann, R. Dörner, and H. Schmidt-Böcking, *Nucl. Instrum. Meth.* A 477, 244 (2002)
7. A. Czasch, J. Milnes, N. Hay, W. Wicking, and O. Jagutzki, *Nucl. Instrum. Meth*. A (2007), in print see also: *http://arxiv.org/abs/physics/0703186*
8. C. Ho, K. L. Albright, A. W. Bird, J. Bradley, D. E. Casperson, M. Hindman, W. C. Priedhorsky, W. R. Scarlett, R. Clayton Smith, J. Theiler, S. Kerry Wilson, *Applied Optic*s 38, 1833 (1999)
9. X. Michalet, O. H. W. Siegmund, J. V. Vallerga, P. Jelinsky, J. E. Millaud, S. Weiss, *Proc. SPIE* 6092, 60920M (2006)
10. V. Emiliani, D. Sanvitto, M. Tramier, T. Piolot, Z. Petrasek, K. Kemnitz, C. Durieux, and M. Coppey-Moisan, *Applied Phys. Lett. 83*, 2471 (2003)
11. V. Dangendorf, G. Laczko, M. Reginatto, D. Vartsky, M. Goldberg, I. Mor, A. Breskin, R. Chechik, *Nucl. Instrum. Meth.* A 542, 197 (2005), see also: *http://www.arxiv.org/abs/physics/0408074*
12. O. Jagutzki, J. S. Lapington, L. B. C. Worth, U. Spillmann, V. Mergel, H. Schmidt-Böcking, *Nucl. Instrum. Meth.* A 477, 256 (2002)
13. J. Barnstedt, M. Grewing, Nucl. Instrum. and Meth. A 477**,** 268 (2002)
14. J. S. Lapington, J. Howorth and J. Milnes, *Proc. SPIE* 5881, 588109 (2005)
15. O. Jagutzki, J. U. Spillmann, L. Spielberger, V. Mergel, K. Ullmann-Pfleger, M. Grewing, H. Schmidt-Böcking, *Proc. SPIE* 3764, 61 (1999)
16. G. Battistoni, P. Campana, V. Chiarella, U. Denni, E. Iarocci, and G. Nicoletti, *Nucl. Instrum. Meth.* 202, 459 (1982)
17. M. S. Dixit, J. Dubeau, J.-P. Martin, K. Sachs, *Nucl. Instrum. Meth.* A 518, 721 (2004)
18. M. S. Dixit, A. Rankin, *Nucl. Instrum. Meth.* A 566, 281 (2006)
19. C. Lu, *Proc. SNIC Symposium*, Stanford (2006) *http://www.slac.stanford.edu/econf/C0604032/papers/0201.PDF*
20. J. H. D. Eland, *Meas. Sci. Technol.* 5, 1501 (1994)
21. see *http://www.roentdek.com*
22. O. Jagutzki, A. Czasch, R. Dörner, M. Hattaß, V. Mergel, U. Spillmann, K. Ullmann-Pfleger, T. Weber, H. Schmidt-Böcking, A. Cerezo, M. Huang, and G. Smith, *IEEE Trans. Nucl. Science* 49, 2477 (2002)
23. V. Dangendorf, G. Laczko, C. Kersten, O. Jagutzki, U. Spillmann, *Proc. of the Seventh World Conference* Vol. 7, 383 (Rome 2002), see also: *http://www.arxiv.org/abs/nucl-ex/0301001*
24. V. Dangendorf, R. Lauck, F. Kaufmann, J. Barnstedt, A. Breskin, O. Jagutzki, M. Kramer, D. Varsky, *Proc. of International Workshop on Fast Neutron Detectors and Applications* (2006), *http://pos.sissa.it//archive/conferences/025/008/FNDA2006_008.pdf*
25. T. Suzuki, S. Gunji, F. Sato, Y. Yamashita, R. Nakajima, H. Sakurai, F. Tokanai, *IEEE Nuclear Science Symposium Conference Record*, Vol.2, 809 (2003)

## ACKNOWLEDGEMENT

The Authors would like to thank Jürgen Barnstedt from the Astronomy Institute of the University in Tübingen, FRG for the provision of an RS-PMT.